

Supporting Information

Photophysical Properties of Octupolar Triazatruxene-Based Chromophores

Guizing He,^a Jinjun Shao,^b Yang Li,^a Jiangpu Hu,^a Huaning Zhu,^a Xian Wang,^a Qianjin Guo,^a Chunyan Chi^{b,*} and Andong Xia^{a,*}

^aBeijing National Laboratory for Molecular Sciences (BNLMS), Key Laboratory of Photochemistry, Institute of Chemistry, Chinese Academy of Sciences, Beijing 100190, People's Republic of China; ^bDepartment of Chemistry, National University of Singapore, 3 Science Drive 3, Singapore 117543, Singapore.

E-mail: andong@iccas.ac.cn; chmcc@nus.edu.sg

S1. Solvation effect: solvent parameters and spectral properties

As shown in Table S1, the spectral properties are found to depend on the solvent polarity. With the increasing polarity of solvents, larger stokes shifts are observed.

Table S1. Solvent parameters, Stokes shifts, and fluorescence quantum yields of chromophores **TAT-Bz**, **TAT-T-Bz** and **TAT-T-PhCN**.

| | parameters | | Stokes shift (cm ⁻¹) | | | Quantum Yield | | |
|-----------------|-------------------------|----------------------|----------------------------------|--------|-------|---------------|--------|-------|
| | Δf ^a | E_T^N ^b | TAT | TAT-Bz | TAT-T | TAT | TAT-Bz | TAT-T |
| | | | | -PhCN | | -Bz | -T-Bz | -PhCN |
| cyclohexane | -0.003 | 0.006 | 3642 | 2332 | 2402 | 0.22 | 0.25 | 0.36 |
| toluene | 0.0159 | 0.099 | 4017 | 2894 | 2759 | 0.17 | 0.25 | 0.38 |
| chloroform | 0.1492 | 0.259 | 5206 | 4556 | 4292 | 0.16 | 0.16 | 0.41 |
| tetrahydrofuran | 0.2103 | 0.207 | 5080 | 4482 | 4592 | 0.20 | 0.21 | 0.40 |
| dichloromethane | 0.2182 | 0.309 | 5998 | 5240 | 5008 | 0.14 | 0.16 | 0.32 |
| acetone | 0.2851 | 0.355 | 6273 | 5599 | 5515 | 0.14 | 0.05 | 0.11 |

^aSolvent polarability: $\Delta f = (\varepsilon - 1) / (2\varepsilon + 1) - (n^2 - 1) / (2n^2 + 1)$

^b $E_T^N = [E_T(30)(\text{solvent}) - 30.7] / 32.4$

Figure S1 shows fluorescence quantum yields of the chromophores in different solvents. In the less polar solvents (less than 0.25), three chromophores show relatively high quantum yield. However, the quantum yields decrease sharply in more polar solvents, which is the character of the ICT compounds.

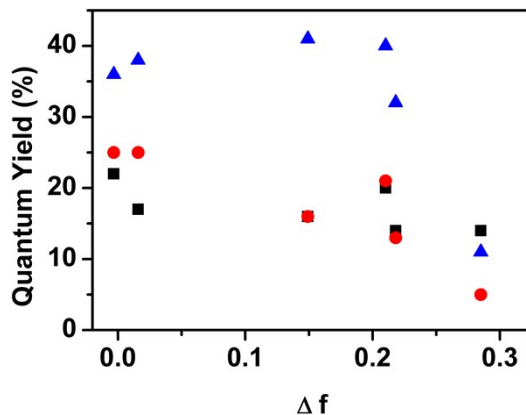


Figure S1. Fluorescence quantum yield versus the polarity of solvents. Black squares, **TAT-Bz**; red circles, **TAT-T-Bz**; blue triangle, **TAT-T-PhCN**

S2. Structures and molecular orbitals of tribranched chromophores

The ground state geometries were optimized using the B3LYP function with the 6-31G(d,p) basis set. Figure S2 shows optimized ground structures and the frontier molecular orbitals of the tribranched chromophores. A stronger polar excited ICT state formed for these compounds compared to their ground state, which plays a significant role in the photophysical properties of these push-pull molecules.

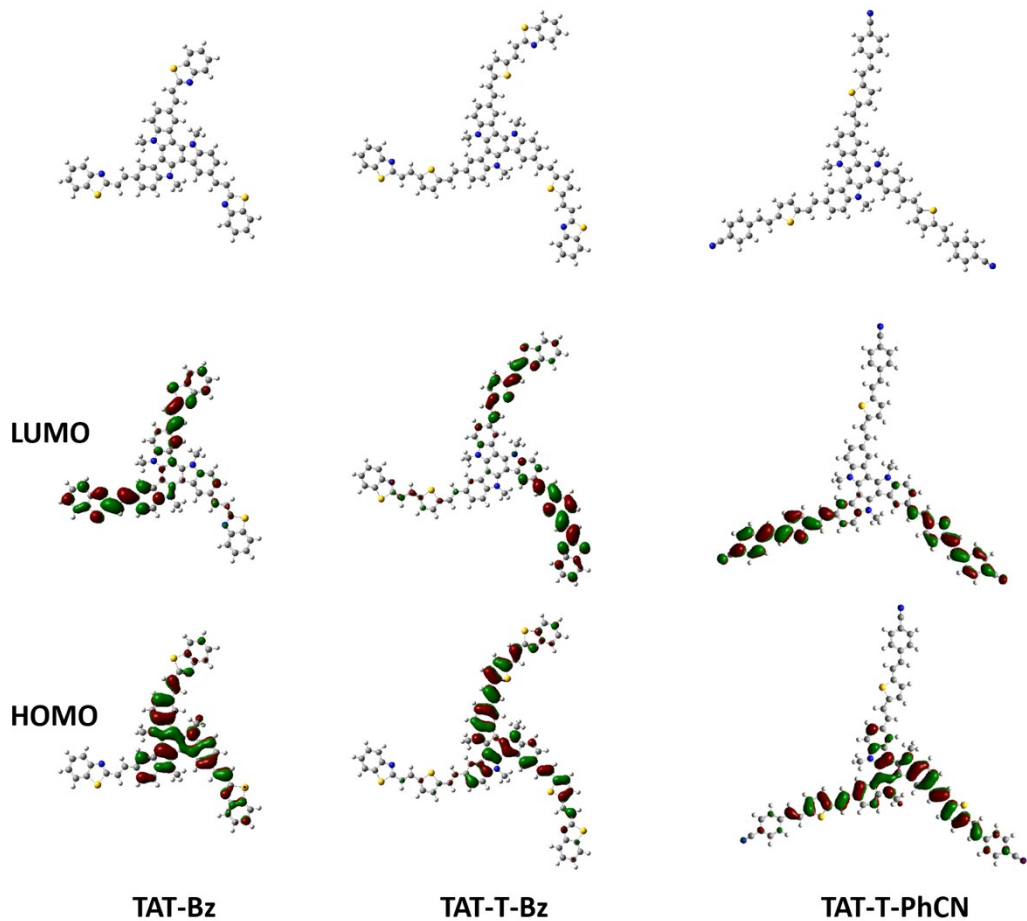
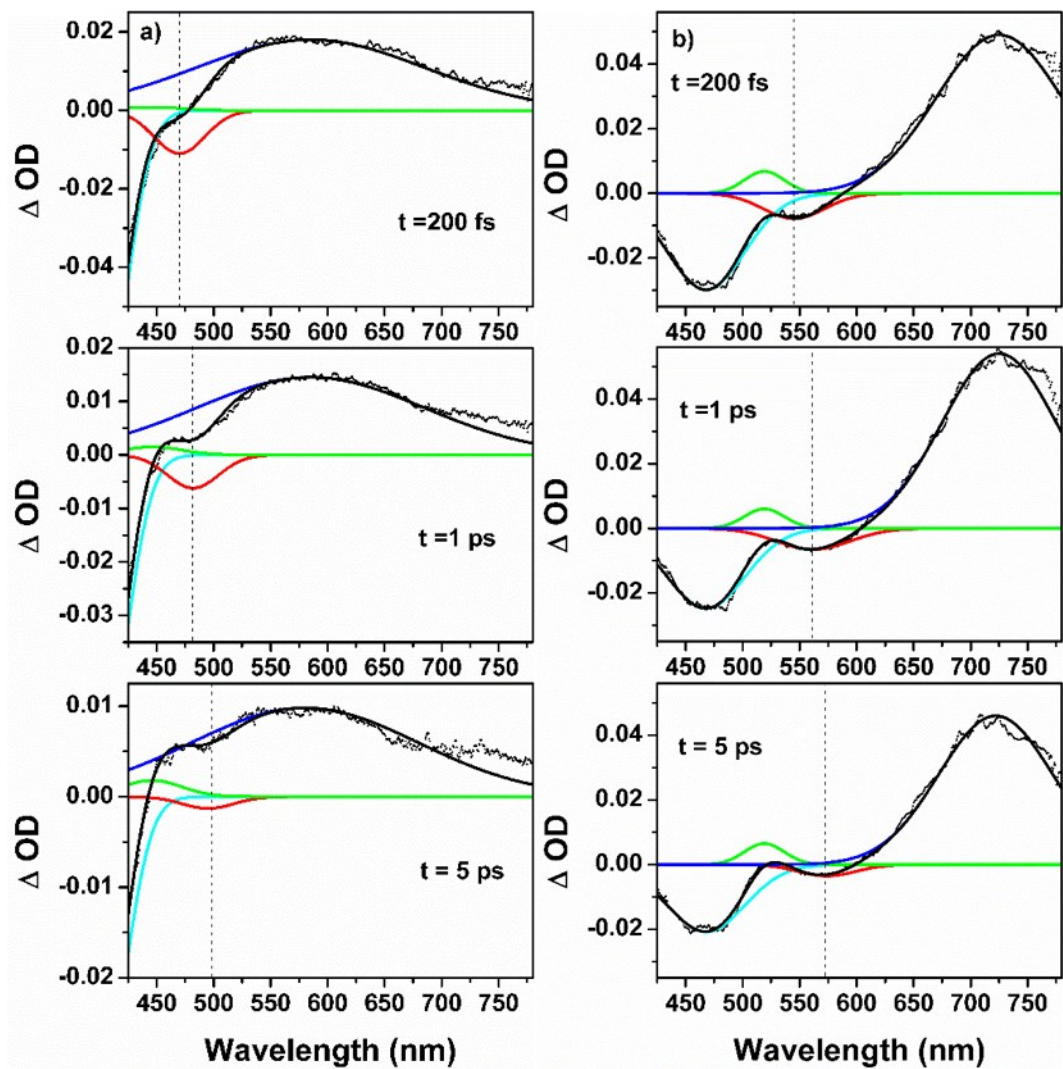


Figure S2. The optimized structures and frontier molecular orbitals of chromophores.

S3. Transient absorption spectra decomposed by Gaussian peaks

Femtosecond broad transient absorption peaks were decomposed using Gaussian peaks (Figure S3). The position of ground-state bleaching (GSB, cyan) was fixed around the peak of steady state absorption during the fitting. Excited-state absorption (ESA) is fitted by two Gaussian peaks, which is slight blue-shift. One is at the short wavelength (green) overlapped with the GSB and SE, another at long wavelength (blue). The decomposing results show a pronounced SE peak shift induced by solvation. Dashed lines are guides for identifying the shift.



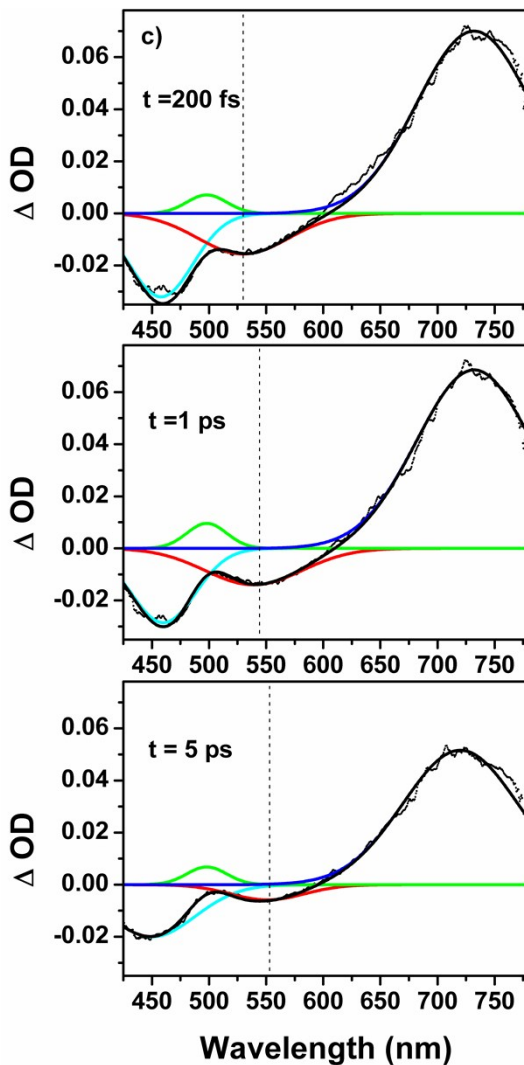


Figure S3. Selected femtosecond transient absorption spectra (black dot) and fits (black line) of chromophores **TAT-Bz** (a), **TAT-T-Bz** (b) and **TAT-T-PhCN** (c) in THF at three example time delays, 200 fs, 1 ps and 5 ps.

S4. Kinetics at selected single wavelengths from femtosecond transient absorption spectra for showing the quality of global fitting

In order to prove the quality of global fitting, kinetics at selected single wavelengths are plotted together with a fit of all the collected time traces in Figure S4, S5 and S6 for the tribranched chromophores **TAT-Bz**, **TAT-T-Bz** and **TAT-T-PhCN**.

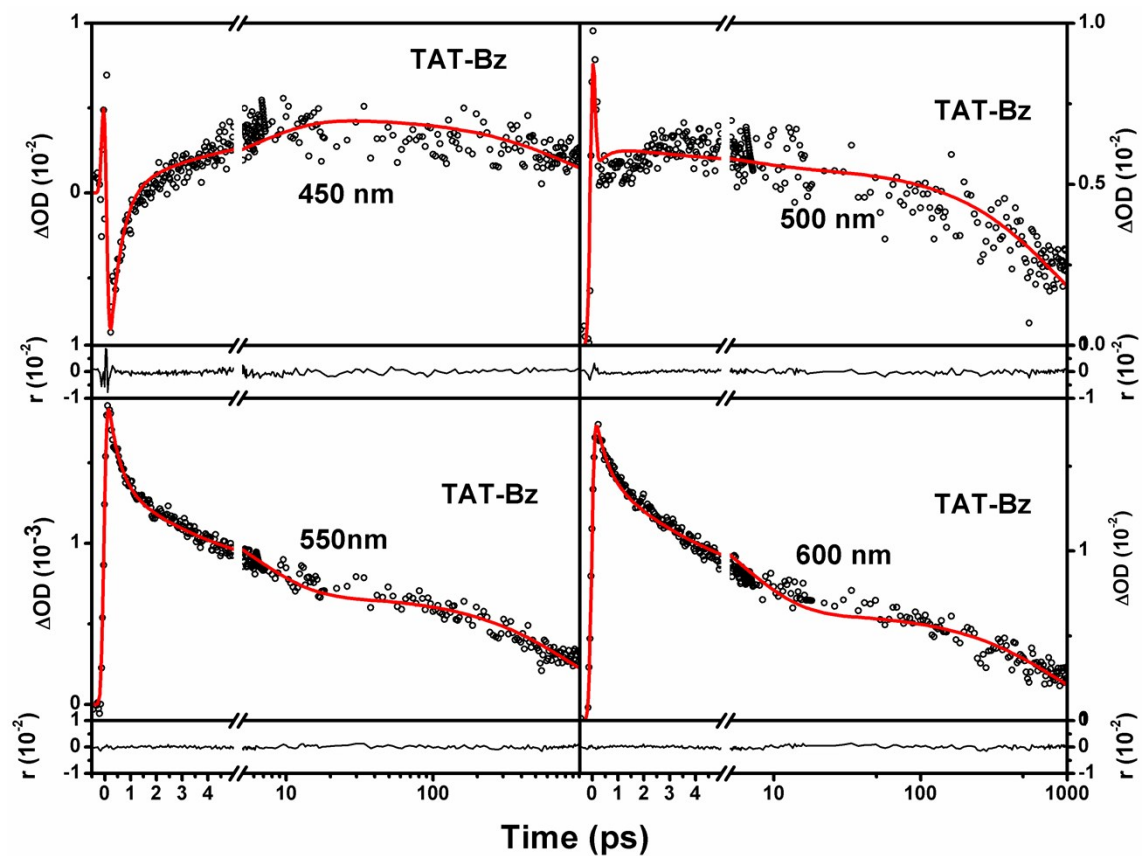


Figure S4. Kinetics at selected single wavelength of TAT-Bz in THF. Fitting curves and residuals of the fitting are also shown. The traces are fitted with the sequential model described in Figure 8a, b and Table 2 in the Text.

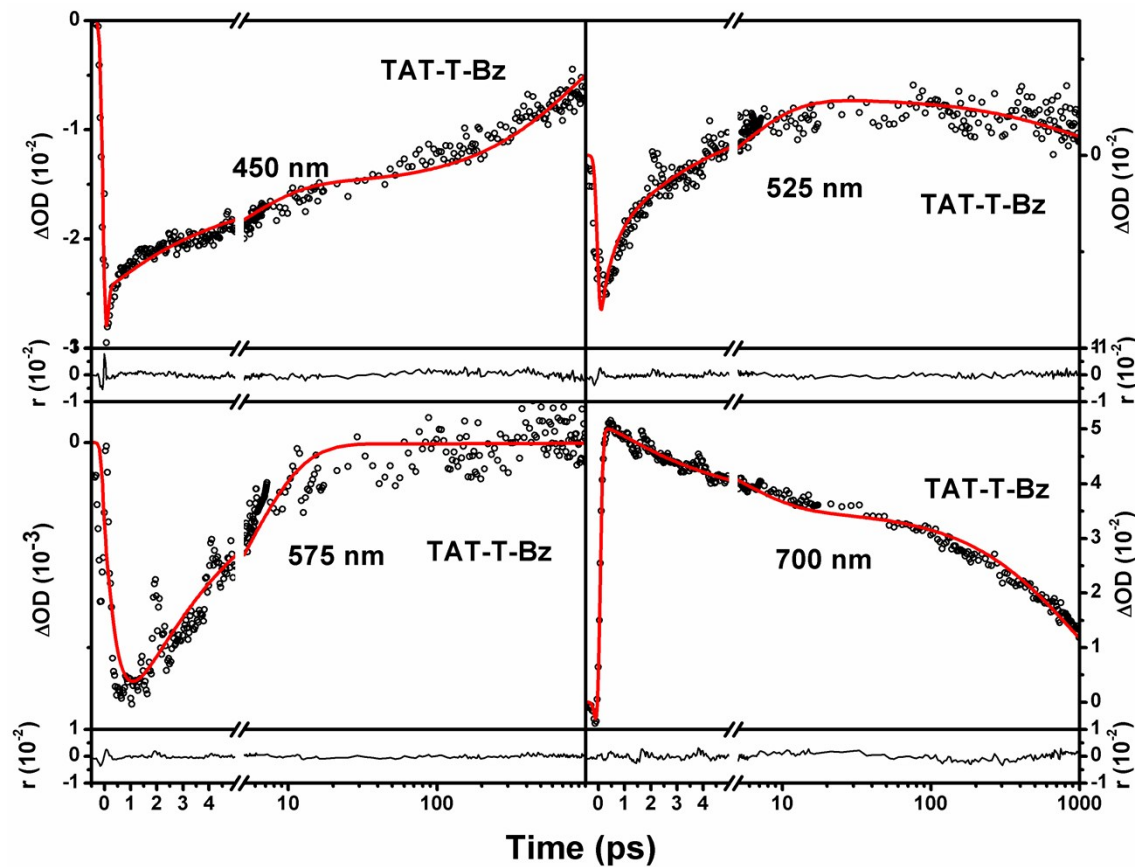


Figure S5. Kinetics at selected single wavelength of TAT-T-Bz in THF. Fitting curves and residuals of the fitting are also shown. The traces are fitted with the sequential model described in Figure 8c, d and Table 2 in the Text.

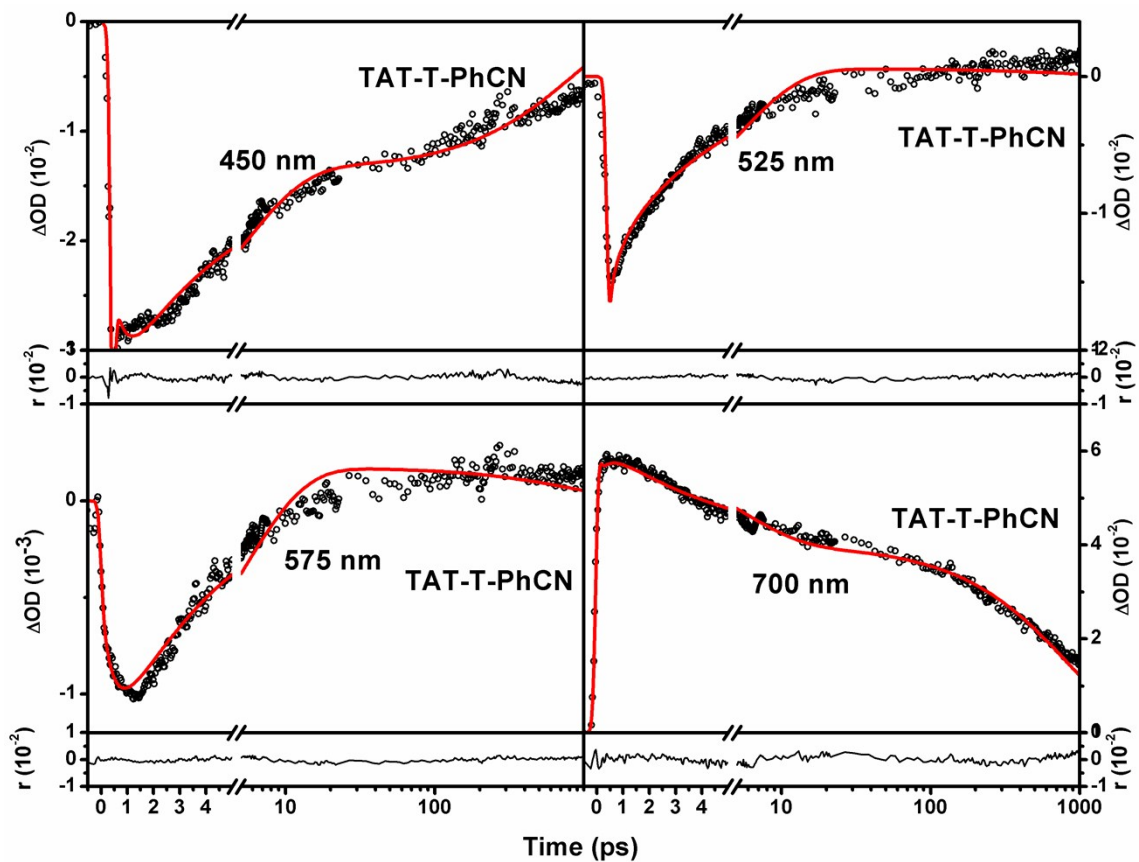


Figure S6. Kinetics at selected single wavelength of TAT-T-PhCN in THF. Fitting curves and residuals of the fitting are also shown. The traces are fitted with the sequential model described in Figure 8e, f and Table 2 in the Text.